Development of a Hard X-Ray Profile Measurement System in the TST-2 Spherical Tokamak

Hiro TOGASHI[a)], Hibiki YAMAZAKI, Akira EJIRI, Yuichi TAKASE, Naoto TSUJII, Satoru YAJIMA, Yusuke YOSHIDA and TST-2 team

The University of Tokyo, Kashiwa 277-8561, Japan

(Received 9 March 2017 / Accepted 3 June 2017)

A compact hard X-ray measurement system was developed to measure bremsstrahlung of fast electrons generated by lower hybrid wave (LHW) in the TST-2 spherical tokamak. The system, which consists of an NaI scintillator, a photomultiplier tube, a curved acrylic lightguide, a lead collimator, and linear and rotational stages, enables us to measure the energy flux profile on the midplane with the energy resolution of 10 - 15 eV at 122 keV and with the energy range from a few tens to several hundreds of keV. Preliminary hard X-ray measurements were performed for LHW-driven TST-2 plasmas, and energy spectra were attained successfully. The typical effective temperature of the spectra is in the order of 10 keV, and we obtained the time evolutions of energy flux and effective temperature with a time resolution of 10 ms. Profile measurement showed that the flux at the inboard side is higher than that at the outboard side.

Keywords: TST-2, spherical tokamak, hard X-ray measurement, lower hybrid wave

DOI: 10.1585/pfr.12.1402030

1. Introduction

One of the issues in the development of a low aspect ratio tokamak reactor is that the optimum current start-up scenario has not been established. Our group has been promoting the establishment of the start-up scenario by lower hybrid wave (LHW) in the TST-2 spherical tokamak device (with major radius $R \sim 0.36$ m, minor radius $a \sim 0.23$ m, toroidal magnetic field $B_t < 0.3$ T, and plasma current $I_p < 25$ kA) [1, 2]. It is recently revealed that fast electrons generated by the LHWs are the dominant pressure component of the TST-2 plasmas [3]. In the evaluation of LHW-driven plasmas, information of hard X-ray (HXR) radiation is important because it reflects the energy of fast electrons and the absorption profile of LHWs and the current density. In addition, effective temperature and energy flux profile of HXR are useful for the analysis of plasma equilibrium and interaction between bulk electrons and fast electrons.

In order to measure HXR radiation due to the fast electrons, an HXR measurement system has been developed in TST-2. The system should have the capability of profile measurement and the sensitive energy range from a few tens to a few hundreds of keV. In TST-2, there are several viewing ports with 3 mm thick borosilicate glass windows with transmissivity of about 60% for a 30 keV HXR photon. However, the diameter of the window is not large because of the thin glass, and the measurable line-of-sight is limited by toroidal field (TF) coils. Therefore, the detection system should be placed inside the TF coils and should be compact to measure the profile. Since we want to measure HXRs with the energies of several hundreds of keV, NaI scintillator is suitable. An avalanche photodiode (APD) and a photomultiplier tube (PMT) are the candidate detectors to measure the scintillation light, but we found an APD is inappropriate due to the large noise level of about 50 keV. Although a PMT has a very high gain, the gain is deteriorated by magnetic fields. We have tested several different scintillators, light transmission schemes and PMTs and their combinations. In this paper, we describe the present system, which satisfies our requirements such as compactness, energy and time resolutions and energy range.

2. Development of a Hard X-Ray Diagnostic System

In order to develop a compact system with a high energy resolution and a wide energy range, a ϕ25.4×25.4 mm NaI scintillator (Type 4B4, OKEN) and a PMT with effective photoelectric surface of ϕ25 (H10426, Hamamatsu photonics) were adopted. In order to mitigate degradation of PMT gain due to magnetic fields, the PMT should be located as far as possible from the device. In the present system, PMT is located at at least 30 cm distance from the TF coil position. It is confirmed that the gain degradation is less than ±1% for the typical coil operation of the TST-2 device. Note that the gain can be deteriorated by 70% when we place the PMT at 10 cm inward side from the TF

author's e-mail: togashi@fusion.k.u-tokyo.ac.jp, hiro.togashi.tm@hitachi.com

a) present address: Hitachi, Ltd., 3-1-1 Saiwai-cho, Hitachi, Ibaraki 317-8511, Japan

coil position.

As a way of transferring the scintillation light, a ϕ25 acrylic lightguide is adopted because a large effective diameter is available despite the cheapness compared with optical fibers. Since a straight lightguide interferes with the TF coils, a lightguide curved by 40 degrees is considered. Firstly, ray tracing simulation was carried out to estimate the transmission efficiency of lightguides. Here, light source is assumed as rays with random starting positions and vectors in the scintillator. The efficiency was calculated for four cases as shown in Fig. 1, i.e., cases (a): without lightguides, (b): with a 220 mm length straight lightguide, (f): with a 220 mm length curved lightguide, and (g): with a 430 mm length curved lightguide used in the plasma measurement. After the calculation, lightguides were prepared and each efficiency was evaluated from the pulse height of Co-57 photoelectron peak (mainly at 122 keV). Here, the reproducibility error of the lightguide setup is about ±1%, and the measurement error is negligible. The results are shown in Table 1, and each efficiency is normalized by that in case (a). Adding a straight lightguide (case (b)), the measured efficiency is 57%. According to the calculation, the deterioration due to the straight lightguide can be explained by the rays, which are not reflected at the the side surface of the lightguide. Furthermore, about 20% of the remaining light are lost by applying the curved lightguide (case (f)). Comparing the calculation results and the measurement results, the measured efficiencies are 1.3 - 1.5 times lower than the calculated ones. Discrepancy of efficiency between them is probably caused by loss at the connection surfaces. On the other hand, the optical loss of about 13% (= 57 - 44%) due to the curvature effect is similar to that in the calculation. PMT is quite sensitive to the light, and it is necessary to shade external light. Cases (c), (d), and (e) in Fig. 1 show straight lightguides with non-adhesive aluminum tape, adhesive aluminum tape, and self-fusing tape, respectively. While the efficiency in case (c) is similar to that in case (b), significant deterioration is found in cases (d) and (e) due to change of refractive index at the side surface of the lightguide. Although the side surface loss is not found in the case with the non-adhesive tape (case (c)), a cylindrical shading container, which has projecting point supports on the inner surface and the contact area is less than 1% of the area, is used in the final system to keep the efficiency high and stable (the optical loss is not found within the error of 1%). Efficiency of case (g) with the lightguide used in the plasma measurement is 39%, and it is still more than ten times higher than the efficiency of the previous system, where a ϕ5 flexible liquid lightguide is used instead of the acrylic lightguide.

Figure 2 shows drawings of the developed system. The system consists of the NaI scintillator, the PMT, the curved acrylic lightguide, lead blocks for shielding, a lead

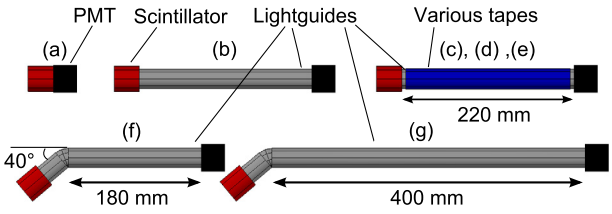

Fig. 1 Types of lightguide used in the tests. Cases (c), (d), and (e) are straight lightguides covered by non-adhesive aluminum tape, adhesive aluminum tape, and self-fusing tape, respectively.

Table 1 Calculated and measured efficiencies in various cases. Each efficiency is normalized by value in case (a).

Type of lightguide used in the tests	Calculated efficiency	Measured efficiency
(a) Without lightguide	100%	100%
(b) Straight lightguide (SL)	72%	57%
(c) SL with aluminum tape	N/A	56%
(d) SL with adhesive tape	N/A	25%
(e) SL with self-fusing tape	N/A	16%
(f) Curved lightguide	60%	44%
(g) Long curved lightguide	59%	39%

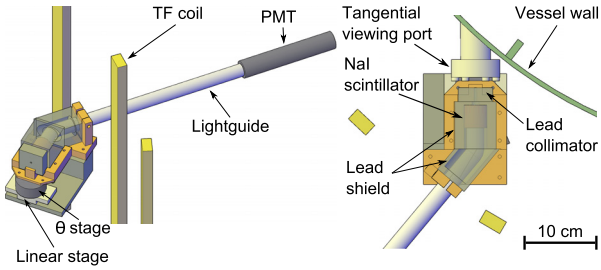

Fig. 2 A schematic drawing of the system installed on TST-2.

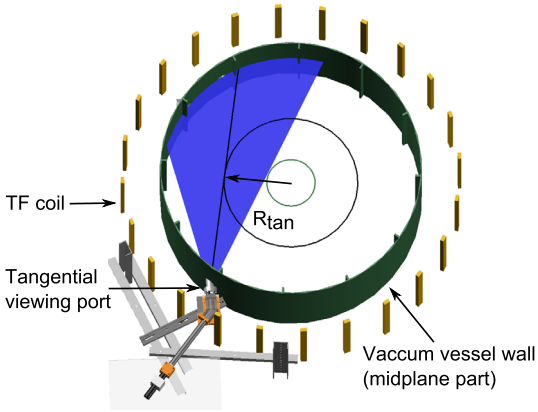

Fig. 3 Definition of tangency radius R_{tan} and measurable range (R_{tan} ≃ 135 - 585 mm) of the developed system.

collimator pinhole ($\phi 5 \times 20$ mm), and theta and linear stages. Many of the components are made by a 3D printer (BS01+, Bonsai Lab.). Measurable energy range is from a few tens to several hundreds of keV, and energy resolution is 10 - 15 eV at 122 keV. The system has a wide line-of-sight angle covering the co-directional part to the plasma current as shown in Fig. 3, and the viewing chord can be set by the two stages. In the line-of-sight range, there are no plasma facing components or antennas which may induce strong thick-target bremsstrahlung radiation. Most part of the scintillator surface is covered by more than 15 mm thick lead blocks, and additional lead blocks along the lightguide reduces HXR entrance from the backside. The collimator pinhole part can be changed depending on the intended use.

3. Hard X-Ray Measurement

HXR measurements were performed for LHW-driven TST-2 plasmas with plasma current up to 11 kA. A $\phi 5$ pinhole with solid angle of 0.049 sr and a lead block without the pinhole were used to check background HXR photons. Figure 4 shows energy spectra for the cases with the pinhole and without the pinhole. HXR photons for 20 - 150 keV were observed successfully in the case with pinhole, and time evolutions of the energy flux and slope of the energy spectrum (i.e., effective temperature) are shown. On the other hand, background level is small, and it is indicated that most of the detected HXR photons come through the pinhole. Here the effect of the window absorption is corrected. Note that the average HXR pulse interval for each time window is longer than 7 μs, and this is much longer than the pulse width (about 0.5 μs), and pile-up effect is negligible in the present measurements.

Figure 5 (a) shows typical plasma current and time evolution of energy flux summed over energy range above 20 keV, and it is indicated that the flux increases with the current. The effective temperature represents the slope of energy spectrum, and its time evolution is shown in Fig. 5 (b). The temperature is in the order of 10 keV throughout the discharge, and it also changes with the current. Errors of the flux and the temperature are about 5% and less than 1%, respectively.

Energy flux profile measurements were performed. Seven reproducible discharges were prepared to scan the viewing chords. A $\phi 3.5$ pinhole with a solid angle of 0.024 sr was used to improve the spatial resolution. The typical resolution is ±60 mm in tangent radius. Figure 6 shows time evolution of energy flux profile summed over energy range above 20 keV. Here, each flux is divided by length of each line-of-sight, of which boundary radius is the same as the limiter position (R = 585 mm). It can be seen that energy flux increases with the current in all the chords, and the flux at the inboard side is higher than that at the outboard side. Note that background measurements without pinhole were performed in all the chords, and it was confirmed that the amount was negligible.

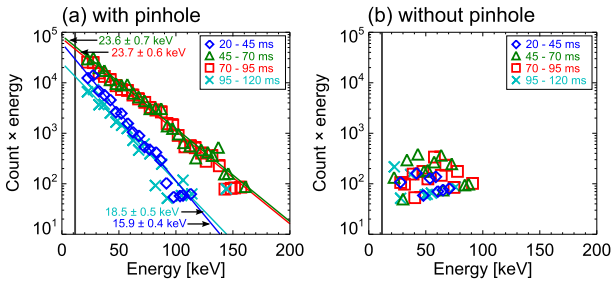

Fig. 4 Energy spectra in the setups with pinhole (a) and without pinhole (b). Each colored line represents the fitting and vertical black line represents the threshold in photon detection. Different symbols represent spectra for different time windows during a discharge. Effective temperatures calculated from linear fitting are shown in the left figure.

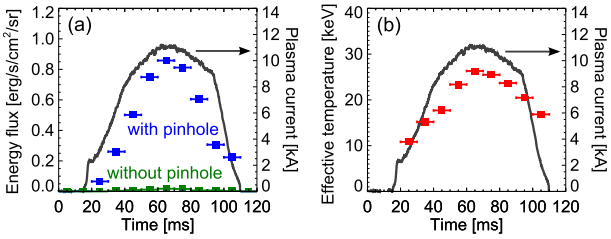

Fig. 5 Time evolution of energy flux with the energy range more than 20 keV for the cases with/without pinhole (a) and effective temperature of fast electrons (b). Plasma current is plotted in both figures (black curve). Horizontal bars represent time windows for each data point.

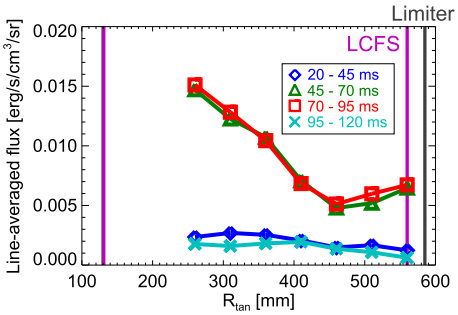

Fig. 6 Time evolution of line-averaged energy flux with the energy range more than 20 keV. Black and purple lines represent locations of limiters and last closed flux surface (LCFS) at the midplane at 60 ms, respectively.

4. Summary

In summary, a compact hard X-ray measurement system with a wide line-of-sight on the midplane and a high energy resolution was developed. HXR measurements were performed for LHW-driven TST-2 plasmas, and time evolution of energy flux and effective temperature were obtained successfully.

Acknowledgments

This work was supported by JSPS Grant-in-Aid for Scientific Research (S) No. 21226021 and (DC2) No. 16J05471, by NIFS Collaborative Research Program Nos. NIFS14KOCR001 and NIFS12KUTR078, and by JSPS A3 Foresight Program 'Innovative Tokamak Plasma Startup and Current Drive in Spherical Torus'.

[1] Y. Takase *et al.*, Nucl. Fusion **41**, 1543 (2001).
[2] T. Shinya *et al.*, Nucl. Fusion **55**, 073003 (2015).
[3] H. Togashi *et al.*, Plasma Fusion Res. **10**, 1202082 (2015).